

Enhancing Sampling Protocol for Robust Point Cloud Classification

Chongshou Li¹, Pin Tang¹, Xinke Li^{*2}, Tianrui Li¹

¹School of Computing and Artificial Intelligence, Southwest Jiaotong University

²National University of Singapore

lics@swjtu.edu.cn, tangpin1874@163.com, xinke.li@u.nus.edu, trli@swjtu.edu.cn

Abstract

Established sampling protocols for 3D point cloud learning, such as Farthest Point Sampling (FPS) and Fixed Sample Size (FSS), have long been recognized and utilized. However, real-world data often suffer from corruptions such as sensor noise, which violates the benignness assumption of point cloud in current protocols. Consequently, they are notably vulnerable to noise, posing significant safety risks in critical applications like autonomous driving. To address these issues, we propose an enhanced point cloud sampling protocol, *PointDR*, which comprises two components: 1) Downsampling for key point identification and 2) Resampling for flexible sample size. Furthermore, differentiated strategies are implemented for training and inference processes. Particularly, an isolation-rated weight considering local density is designed for the downsampling method, assisting it in performing random key points selection in the training phase and bypassing noise in the inference phase. A local-geometry-preserved upsampling is incorporated into resampling, facilitating it to maintain a stochastic sample size in the training stage and complete insufficient data in the inference. It is crucial to note that the proposed protocol is free of model architecture altering and extra learning, thus minimal efforts are demanded for its replacement of the existing one. Despite the simplicity, it substantially improves the robustness of point cloud learning, showcased by outperforming the state-of-the-art methods on multiple benchmarks of corrupted point cloud classification. The code will be available upon the paper's acceptance.

1 Introduction

In the rapidly evolving field of 3D data perception via deep learning (Qi et al. 2017a,b; Guo et al. 2020), point cloud sampling serves as a critical component in the standard learning and recognition pipeline (Hu et al. 2020; Qian et al. 2022; Yu et al. 2022; Zhang et al. 2022b). Following the legacy of pioneer works (Qi et al. 2017a,b), existing sampling protocols are primarily designed and optimized for clean data, without taking into account corruptions. However, due to the high complexity of real-world, point cloud data are almost always incomplete and with noise in practice (Ren et al. 2022), posing threats to 3D deep learning applications. For example, noisy background points or slight perturbations generated by inaccurate processing or sensor

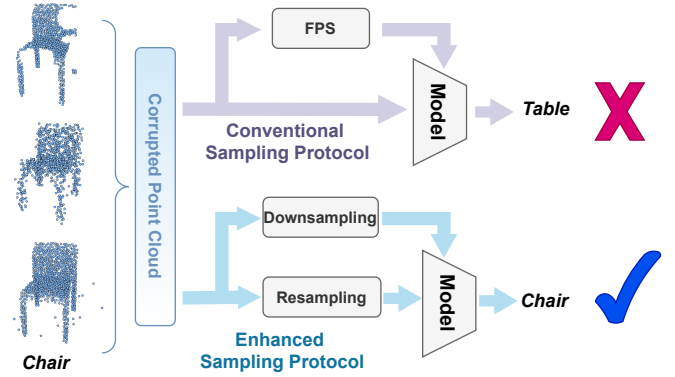


Figure 1: The well-established existing sampling protocol is not optimized for corrupted point cloud in practice. To address the robustness issue, we propose to enhance the protocol by revising the farthest point sampling (FPS) into new downsampling and integrating resampling into process.

error can significantly decrease the deep model performance (Ren et al. 2022; Sun et al. 2022). Such performance drops can lead to serious safety consequences, especially in critical 3D applications like autonomous driving. Therefore, it is necessary to rethink and redesign point cloud sampling protocols with a focus on robustness against corruptions to ensure reliable 3D deep learning in real-world conditions.

One crucial limitation of established sampling protocols is that they are sub-optimal under the corrupted data distribution. For instance, the protocol samples a fixed number of points in data preparation, namely, Fixed Sample Size (FSS) (Qi et al. 2017a). This convention overlooks the facts that point clouds in the real world naturally vary in size and density. These varied sizes are even obvious in particular corruptions such as occlusions and density-related noise (Sun et al. 2022; Ren et al. 2022). Another aspect is that the widely used Farthest Point Sampling (FPS) (Eldar et al. 1997) for key points selection is especially vulnerable to outliers due to its inherent basis of Euclidean distance and sensitivity to sparse points (Yan et al. 2020). Several works have considered updating a specific step to deal with this issue, like PointASNL (Yan et al. 2020) and ADS (Hong, Chou, and Liu 2023). The learning-based methods put extra

*Corresponding author

effort into module training and may be potentially overfitting. Overall, none of them propose a comprehensive and alternative solution to overcome the sampling protocol limitations.

To overcome these limitations, we propose an enhanced point cloud sampling protocol, **PointDR**, by revising the **Downsampling** process and integrating **Resampling** process before inputting, as illustrated in Figure 1. The implementation of the proposed protocol involves randomizing the sampling during training and processing noisy point clouds during inference. To achieve this, the downsampling process assisted by point reweighting is applied to ensure that potential outliers are not captured as key points. The point weight is named as isolation rate evaluating the extent of local isolation for a point. Moreover, the proposed resampling process randomizes the sample size during training; and restores insufficient point clouds in the inference stage. Inspired by shape-invariant perturbation (Huang et al. 2022), we realize the upsampling of resampling process via a tangent plane interpolation technique that enhances the density of point cloud data while preserving local geometry. Overall, the enhanced sampling protocol is learning-free thus straightforward to implement and can be seamlessly integrated into the existing point cloud analysis pipeline.

Our contributions are summarized as follows:

- We first comprehensively revisit the long-existing sample protocol for point cloud learning through the lens of data corruption. Based on the analysis, we propose an alternative protocol to enhance the robustness of point cloud learning.
- We develop two learning-free techniques as the key of protocol, namely, point reweighting and tangent plane interpolation, which can deal with point cloud corruption in different aspects. The whole proposed protocol is free of model architecture change and extra learning, thus it can be implemented to replace the current protocol with minimal pains and fits almost all 3D deep models.
- Extensive experiments are conducted on multiple corrupted 3D point cloud datasets. The results have demonstrated that the proposed protocol is able to improve the robustness of 3D point cloud classification and outperform the latest methods.

2 Related Work

Point Cloud Sampling. Point cloud sampling techniques typically consist of: 1) downsampling, also known as “simplification” (Dovrat, Lang, and Avidan 2019), and 2) upsampling (Zhang et al. 2022b). These techniques are divided into non-learning-based and learning-based methods (Zhang et al. 2022b). Traditional non-learning-based downsampling techniques include Farthest Point Sampling (FPS) (Eldar et al. 1997), Random Sampling (RS) (Hu et al. 2020), Poisson Disk Sampling (PDS) (Ying et al. 2013), and voxelization (Lv, Lin, and Zhao 2021). Conversely, learning-based downsampling methods account for downstream tasks (Dovrat, Lang, and Avidan 2019; Lang, Manor, and Avidan 2020; Nezhadarya et al. 2020; Qian et al. 2020, 2023). Upsampling is categorized into learning-based (Yu et al.

2018b,a; Yifan et al. 2019; Dai et al. 2020; Ye et al. 2021; Qiu, Anwar, and Barnes 2022; He et al. 2023a,b) and non-learning-based approaches (Alexa et al. 2003; Lipman et al. 2007; Huang et al. 2009, 2013; Wu et al. 2015a). The non-learning-based sampling techniques are particularly susceptible to outliers due to their inherent structural limitations; meanwhile, the learning-based methods are either also sensitive to noise or dependent on downstream tasks and prone to overfitting. This paper introduces simple yet effective robust point cloud sampling techniques to overcome these challenges.

Point Cloud Robust Classification. PointNet (Qi et al. 2017a) has been a trailblazer in utilizing deep learning for point cloud analysis, with notable extensions such as PointNet++ (Qi et al. 2017b), GDANet (Xu et al. 2021), Point Transformer (PCT) (Guo et al. 2021), and CurveNet (Xiang et al. 2021). However, the performance of these models significantly deteriorates with corrupted real-world data (Uy et al. 2019; Ren et al. 2022; Sun et al. 2022). To tackle this issue, existing literature offers three main types of solutions. The first focuses on modifying the model by altering its structure or training strategies, such as pooling operations based on sorting (Sun et al. 2020) and model aggregation (Dong et al. 2020). The second type includes certified methods, exemplified by Pointguard, which theoretically enhances model robustness through certified classification (Liu, Jia, and Gong 2021). The third type is data-driven approaches that directly cleanse corrupted data, with notable methods including IF-defense (Wu et al. 2020) and DUP-Net (Zhou et al. 2019). This paper aims to advance robustness from a new perspective by refining point cloud sampling protocol during data preparation.

Point Cloud Augmentation. Point cloud augmentation is a widely recognized practice in the deep learning community, employed to improve the generalization capabilities of neural networks. Traditional augmentation methods, including random scaling, rotation, and jitter, are somewhat limited in their effectiveness for point cloud analysis (Zhu, Fan, and Weng 2024). Recent advancements have introduced sophisticated techniques such as PointCutMix (Zhang et al. 2022a), PointAugment (Li et al. 2020), PointMixup (Chen et al. 2020), and PointWOLF (Kim et al. 2021). However, they suffer from various limitations. For instance, while PointMixup (Chen et al. 2020) and PointWOLF (Kim et al. 2021) largely rely on predefined transformations, PointAugment (Li et al. 2020) emphasizes global transformations, often at the expense of local geometric details. To our knowledge, the sampling augmentation of point cloud for robust classification has been largely unexplored. In this work, we aim to enhance sampling protocols specifically tailored for robust point cloud classification, addressing this critical gap.

3 Proposed Sampling Protocol

3.1 Existing Protocol for Noisy Point Cloud

Mainstream 3D classification models follow the protocol focusing on a clean point cloud with a fixed sample size. Formally, they consider an input of a point cloud $\mathcal{P} = \{\mathbf{p}_i\}_{i=1}^N$, where $\mathbf{p}_i \in \mathbb{R}^3$ and N is the fixed number of points. Specif-

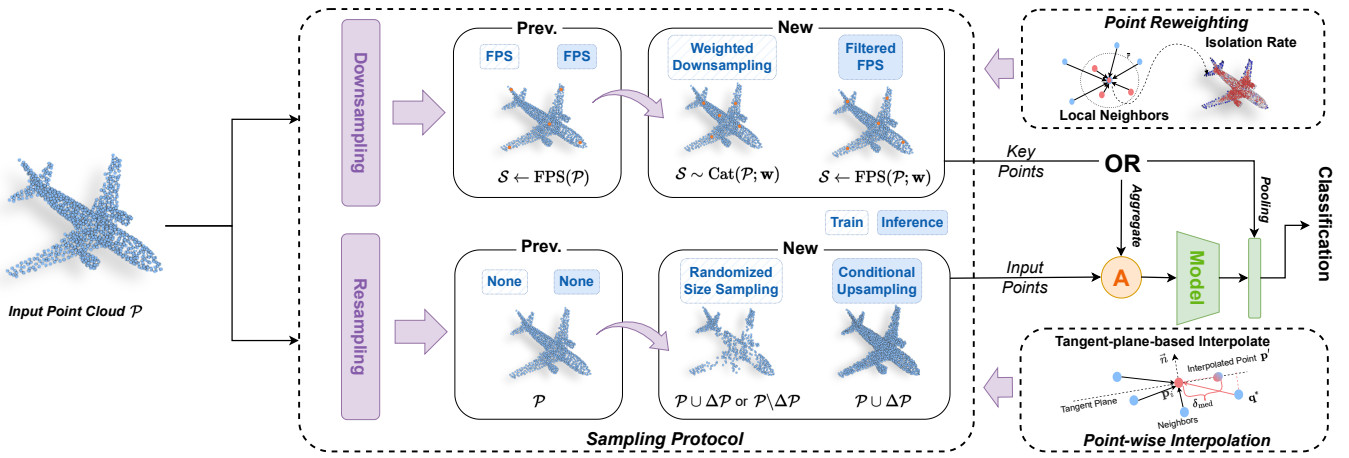


Figure 2: PointDR: enhanced protocol of point cloud sampling for robust classification. The existing protocol used farthest point sampling (FPS) and non-processed points for input. In our protocol, weighted downsampling (WD) and random masking are utilized in training to conduct sampling-based data augmentation. During testing, filtered FPS (FFPS) is implemented to avoid outliers, and an upsampling strategy is used to densify sparse input. Particularly, we propose the concept of isolation rate and the algorithm of tangent plane interpolation to obtain point weights and upsampled points, respectively.

ically, this existing protocol used farthest point sampling (FPS) to select key points from \mathcal{P} as anchors and no further processing for input. FPS is achieved by updating a subset $S \subseteq \mathcal{P}$ with the points s_t iteratively, given by

$$s_t = \arg \max_{\mathbf{p}_i \in \mathcal{P}} \min_{\mathbf{s} \in S} \|\mathbf{p}_i - \mathbf{s}\|_2, \quad (1)$$

where t is the iteration time.

However, in this work, we consider real-world applications, where point clouds are always noisy and with non-fixed sample size. A noisy point cloud \mathcal{P}' can be formulated by

$$\mathcal{P}' = \mathcal{P} \setminus \mathcal{P}_s \cup \mathcal{O} \quad (2)$$

where \mathcal{P}_s is the subset of clean point cloud \mathcal{P} and \mathcal{O} is the added noise points, *i.e.*, outliers. For instance, they could be caused by occlusion and sensor error (Sun et al. 2022), respectively. The formulation (2) indicates the robustness issue of the current sampling protocol working on noisy point clouds from three aspects:

- The presence of outliers \mathcal{O} could affect model trained on outlier-free data. In addition, FPS is essentially sensitive to outliers since Eq. (1) tends to sample far and sparse points.
- The subtraction of \mathcal{P}_s from \mathcal{P} results in a loss of information for model input. There is no counterpart mechanism against it in the current protocol.
- The uncertainty in sample size of both \mathcal{P}_s and \mathcal{O} introduces variability in the final point number of \mathcal{P}' , which violates fixed-number input in current sampling.

Overall, the above issues are evident in recent works (Ren et al. 2022; Sun et al. 2022) demonstrating the unideal performance of conventional sampling protocol against point cloud corruption. To overcome the issues, we attempt to revise the protocol for robust point cloud learning.

3.2 Proposed Sampling Techniques

Before proposing the new sampling protocol, we introduce two key techniques of point cloud sampling.

Point Reweighting. The point-wise weight can be defined by the concept of *Isolation Rate*. At first, we calculate the radius of a sphere containing k nearest neighbors of each point in \mathcal{P} , which is given by,

$$r_i = \max_{\mathbf{q}_j \in \mathcal{N}_i^k} \|\mathbf{p}_i - \mathbf{q}_j\|_2 \quad (3)$$

where $\mathcal{N}_i^k \subseteq \mathcal{P}$ is the set of k neighbors of i -th point \mathbf{p}_i . We further define *Isolation Rate* for each point as w_i , given by,

$$w_i = \Pr_{d \in \mathcal{D}_i} (d \leq \bar{r}), \mathcal{D}_i = \{\|\mathbf{q}_j - \mathbf{p}_i\|_2 : \forall \mathbf{q}_j \in \mathcal{N}_i^k\} \quad (4)$$

where $\bar{r} = \text{Median}(\{d_i\}_{i=1}^N)$ is the median of all radius and $\Pr_Y(X)$ is the probability of X given condition Y . The isolation rate of a point suggests the extent of a point being isolated, *i.e.*, far from others in a probability way. Although a few associated concepts were proposed to calculate the exact local radius of points (Sotoodeh 2006) and identify outliers, the isolation rate is naturally fit for point weighting due to the probability representation. We apply it in our downsampling stage of the proposed protocol.

Local-geometry-preserved Interpolation. A learning-free interpolation algorithm is proposed for our new sampling protocol. The algorithm's objective is to densify the current point cloud while preserving the local geometry of each point. To achieve this purpose, we meticulously interpolate each point and its neighbor, confining the interpolation on the tangent plane. The precise step is outlined in Algorithm 1, with mathematical details provided in Supplementary materials. This tangent-plane-based interpolation approach ensures that the upsampled point cloud retains the

local geometry, *i.e.*, the normals of the point, while integrating local neighborhood information, thereby augmenting its informational richness.

Algorithm 1: Local Geometry Preserved Interpolation

Require: Point cloud \mathcal{P} , Point cloud normal $\{\mathbf{n}_i\}_{i=1}^N$, A query point $\mathbf{p}_i \in \mathcal{P}$, Integer k

Ensure: A new point \mathbf{p}'_i

- 1: $\mathcal{N}^k \leftarrow k\text{NN}(\mathcal{P}, \mathbf{p}_i, k)$ $\triangleright k$ nearest neighbors of \mathbf{p}_i
 - 2: $\delta_{\text{med}} \leftarrow \text{Median}(\{\|\mathbf{p}_i - \mathbf{q}\| : \mathbf{q} \in \mathcal{N}^k\})$ \triangleright Compute the median of local distances as interpolation norm.
 - 3: $\mathbf{q}^* \sim \mathcal{N}^k$ \triangleright Sample a random neighbor
 - 4: $\mathbf{v}_i \leftarrow (\mathbf{I} - \mathbf{n}_i \mathbf{n}_i^\top) \cdot (\mathbf{q}^* - \mathbf{p}_i)$ \triangleright Compute the interpolation direction on tangent plane.
 - 5: $\mathbf{p}'_i \leftarrow \mathbf{p}_i + \delta_{\text{med}} \frac{\mathbf{v}_i}{\|\mathbf{v}_i\|}$ \triangleright Create interpolated point
 - 6: **return** \mathbf{p}'_i .
-

3.3 PointDR: Enhanced Sampling Protocol

Based on the above techniques, we propose the enhanced sampling protocol, PointDR, including resample and down-sample protocols.

Resampling Protocol. During the inference stage, we incorporate the upsampling into preprocessing when the input sample size is insufficient. Given an input point cloud \mathcal{P} , we implement $\mathcal{P} \cup \Delta\mathcal{P}$ if $|\mathcal{P}| < N$. Here $\Delta\mathcal{P}$ is generated by performing Algorithm 1 on $N - |\mathcal{P}|$ points of \mathcal{P} . During the training of point cloud processing models, we randomize the number of points in the training data. In particular, we sample $N + \Delta N$ points from the original N -size point cloud \mathcal{P} , where ΔN is a random variable given by $\lceil 2^{\mathbb{U}[-1,1]} \cdot N - N \rceil$ with continuous uniform distribution $\mathbb{U}[\cdot, \cdot]$. The sign of ΔN indicates distinctive strategies of resampling, namely point adding and dropping, given by

$$\tilde{\mathcal{P}} = \begin{cases} \mathcal{P} \cup \Delta\mathcal{P} & \Delta N > 0, \\ \mathcal{P} \setminus \Delta\mathcal{P} & \Delta N < 0. \end{cases} \quad (5)$$

where $\tilde{\mathcal{P}}$ is the resampled point cloud and $\Delta\mathcal{P}$ is sampled by

$$\Delta\mathcal{P} \sim \begin{cases} \{\Gamma : \Gamma \subseteq \mathcal{U}, |\Gamma| = \Delta N\} & \Delta N > 0, \\ \{\Gamma : \Gamma \subseteq \mathcal{N}_i^k, |\Gamma| = -\Delta N\} & \Delta N < 0, \end{cases} \quad (6)$$

where \mathcal{U} is the point-wise upsampled \mathcal{P} by Algorithm 1, and \mathcal{N}_i^k is the k -NN points of a random center \mathbf{p}_i with $\tilde{k} \sim \mathbb{U}[|\Delta N|, N]$. This stochastic strategy aims to enhance the model's adaptability, given that point cloud data in real-world scenarios inherently exhibit non-fixed variable sizes.

Downsampling Protocol. Recall the iteration rule of FPS in Equation (1), which is sensitive to outliers. To address the issue, during the inference stage, we incorporate point weights to modify the equation into a weighted version,

$$\mathbf{s}_t = \arg \max_{\mathbf{p}_i \in \mathcal{P}} w_i \min_{\mathbf{s} \in S_t} \|\mathbf{p}_i - \mathbf{s}\|_2. \quad (7)$$

This formulation introduces a new objective into FPS downsampling, which is suppressing the selection of points with high weights. In practice, we binarize the point weights via a quantile-based threshold ω (*e.g.*, ω is 0.95 quantile of

$\{w_1, \dots, w_N\}$) and replace the continuous weights. We empirically find that the binary weights are easy to integrate with FPS implementation and show a better performance. The binarized version method is called *Filtered FPS* (FFPS). During the training stage, we perform weighted downsampling (WD) by stochastic subset selection, namely,

$$\mathbf{s}_t \sim \text{Cat}(\mathcal{P}; \mathbf{w}), \quad (8)$$

where $\text{Cat}(\cdot; \cdot)$ is the categorical distribution, and $\mathbf{w} = \{w_1, \dots, w_N\}$. In addition, we extend the downsampling method to 3D models free of key point selection operations, like GDANet (Xu et al. 2021). In this case, We simply replace the pooling operation on features of the whole point cloud by pooling on the downsample-selected subset.

Computational Cost. We design the sampling protocol in the way that poses minimal computational effort beyond the original protocol. Particularly, the implementation of FPS in conventional protocol involves the calculation of point paired distances with complexity of $O(N^2)$. The proposed point reweighting and interpolation (for all points) techniques can utilize the same paired distances and induce extra operations with $O(kN)$ complexity. Such extra computation effort is minor since $k \ll N$. More experimental results of computational costs are presented in Appendix.

4 Experimental Studies

4.1 Experimental Setup

Dataset and Model. We utilize models trained on ModelNet40 (Wu et al. 2015b) to conduct experiments on three corrupted datasets: ModelNet40-C, PointCloud-C, and OmniObject-C. The ModelNet40-C (Sun et al. 2022) and PointCloud-C (Ren et al. 2022) are datasets applying 15 and 7 distinct corruptions to ModelNet40's test set, totaling 2,468 objects. The OmniObject-C, based on OmniObject3D (Wu et al. 2023), has 362 objects corrupted by the methods proposed in (Ren et al. 2022). For 3D deep models, we employ PointNet (Qi et al. 2017a), PointNet++ (Qi et al. 2017b), GDANet (Xu et al. 2021), CurveNet (Xiang et al. 2021), PCT (Guo et al. 2021), following the pipeline in ModelNet40-C including batch size and training protocol. We note that all experiments are run on NVIDIA GeForce RTX 3090 GPUs.

Parameters Setting. The number of nearest neighbors k used in point weight computation is set to 20, which follows the common setup. During the inference phase, the downsampling protocol applies a threshold ω of 0.95, exploring the learning as depicted in Figure 3, meaning that FFPS filters out points within the lowest 5% of point weights.

Evaluation Protocol. We report the error rates (ER) and mean error rates (mER) across multiple corruptions on the three corrupted datasets for performance evaluation. A smaller ER indicates a superior performance. More implementation details are referred to Appendix.

4.2 Main Results

Overall Results. Mean error rates (mERs) for the three corrupted datasets are presented in Table 1. To facilitate a comprehensive comparison, we include multiple baseline models. The results clearly indicate that the proposed PointDR

significantly enhances PCT and CurveNet; mERs decrease by approximately 10% across all datasets, with the most substantial improvement observed in PointCloud-C.

Method	MNC	PCC	OmniC
PointNet (Qi et al. 2017a)	28.3	33.7	65.2
PointNet++ (Qi et al. 2017b)	30.6	27.7	73.9
DGCNN (Wang et al. 2019)	25.9	23.5	73.7
RSCNN (Liu et al. 2019)	26.2	26.1	72.4
CurveNet (Xiang et al. 2021)	23.1	24.4	67.9
SimpleView (Goyal et al. 2021)	27.2	24.3	71.8
GDANet (Xu et al. 2021)	23.5	24.6	70.9
PCT (Guo et al. 2021)	25.5	25.8	69.8
PCT+PointDR	15.8	12.5	60.8
CurveNet+PointDR	15.8	13.7	57.9

Table 1: Mean error rate (mER) across all corruptions of popular 3D deep models w/o our protocol on three datasets. The best mERs are highlighted in bold. MNC, PCC and OmniC represent ModelNet40-C, PointCloud-C and OmniObject-C, respectively.

Results on ModelNet40-C. Extensive evaluations of PointDR on ModelNet40-C utilizing five 3D deep models revealed its superiority. Compared to five enhancement techniques (CutMix-R (Zhang et al. 2022a), CutMix-K (Zhang et al. 2022a), Mixup (Chen et al. 2020), Rsmix (Lee et al. 2021), and PGD (Sun et al. 2021)), PointDR significantly improved all models except PointNet, where it ranked second. Across corruption types, PointDR consistently achieved the lowest error rates: 24.1% for “Density”, 9.5% for “Noise”, and 11.1% for “Transformation”, demonstrating robustness. Notably, its unique randomized size sampling in resampling and FFPS in downsampling effectively tackled “Density” and “Noise” corruptions, enhancing resilience and eliminating outliers, respectively. Detailed corruption results are provided in the Appendix.

Results on PointCloud-C. Table 3 presents the results on the PointCloud-C dataset, emphasizing the robustness of PointDR in enhancing point cloud classification accuracy under various corruption scenarios, outperforming other state-of-the-art augmentation methods. Notably, under specific additive corruption types, our FFPS technique achieves an impressive error rate of 7.5%, likely attributed to the weights utilized by FFPS that effectively filter out outliers. However, it is crucial to note that under the “Jitter” corruption, PointDR does not attain optimal performance, where the PGD strategy excels, probably due to its unique optimization mechanism that better guides the model to learn robust features under subtle perturbations. Furthermore, for drop-type corruptions, the CutMix and Rsmix methods exhibit greater robustness, potentially because their strategies of mixing or replacing data segments enhance the model’s tolerance to local or global information loss. Additional results can be found in the Appendix.

Results on OmniObject-C. Table 4 compares mER on OmniObject-C between PointDR and various state-of-the-art point cloud enhancement methods across three 3D deep models. Results highlight PointDR’s effectiveness in boost-

Method	mER	Density	Noise	Trans
PointNet	28.3	28.3	32.7	24.0
+ CutMix-R	21.8	30.5	<u>18.0</u>	16.9
+ CutMix-K	<u>21.6</u>	26.8	21.8	16.3
+ Mixup	25.4	28.3	28.9	19.0
+ Rsmix	22.5	<u>24.8</u>	27.3	<u>15.5</u>
+ PGD	25.9	28.8	28.4	20.5
+ PointDR	<u>21.6</u>	26.0	18.6	20.2
PointNet++	30.6	36.9	30.3	24.6
+ CutMix-R	19.8	26.8	14.0	18.6
+ CutMix-K	21.3	24.9	19.3	19.6
+ Mixup	18.6	29.7	<u>12.6</u>	<u>13.5</u>
+ Rsmix	27.0	28.9	23.8	28.3
+ PointDR	<u>17.7</u>	24.1	12.7	16.2
GDANet	23.5	33.2	23.7	13.7
+ CutMix-R	16.9	28.5	10.4	<u>11.9</u>
+ CutMix-K	17.8	28.8	12.6	<u>11.9</u>
+ Mixup	18.5	30.3	13.1	12.2
+ Rsmix	19.2	<u>27.7</u>	14.4	15.4
+ PGD	20.3	32.1	15.9	13.0
+ PointDR	<u>16.8</u>	28.3	<u>10.0</u>	12.1
CurveNet	23.1	31.4	26.5	<u>11.4</u>
+ CutMix-R	16.1	25.7	10.5	12.1
+ CutMix-K	17.1	<u>24.8</u>	13.6	12.9
+ Mixup	20.8	32.4	17.9	12.1
+ Rsmix	19.9	26.7	15.6	17.3
+ PGD	20.4	28.5	21.3	<u>11.4</u>
+ PointDR	15.8	25.6	<u>10.2</u>	11.7
PCT	25.5	34.8	28.1	13.5
+ CutMix-R	16.3	27.1	10.5	11.2
+ CutMix-K	16.5	25.8	12.6	11.1
+ Mixup	19.5	30.3	16.7	11.5
+ Rsmix	17.3	<u>25.0</u>	12.0	15.0
+ PGD	18.4	29.3	14.7	11.1
+ PointDR	15.8	26.9	9.5	11.1

Table 2: Comparison of mean error rate (mER) on ModelNet40-C between PointDR and state-of-the-art point cloud enhancement methods across five 3D deep models. The best mERs for each 3D deep model are underlined. Trans refers to the Transformation Corruptions.

ing OOD robustness (Wu et al. 2023). PointDR attains lowest mER for CurveNet (57.9%) and best in “Jitter” (61.4% mER). For PointNet++, it excels in “Drop-G” and “Add-G”. For PCT, PointDR is highly competitive, achieving the best results concurrently with Cutmix-R.. Overall, results validate PointDR’s exceptional OOD generalization. Further implementation details and additional results for PointNet and GDANet are referred to the Appendix.

4.3 Ablation Studies

In the ablation studies, we use PCT (Guo et al. 2021) and CurveNet (Xiang et al. 2021) as 3D deep models on two datasets: ModelNet40-C (Sun et al. 2022) and PointCloud-

Method	mER	Scale	Jitter	Drop-G	Drop-L	Add-G	Add-L	Rotate
PointNet++	27.7	9.4	50.3	26.2	39.6	15.9	20.2	32.5
+ CutMix-R	17.5	8.8	34.5	9.0	20.9	<u>7.7</u>	<u>8.1</u>	33.7
+ CutMix-K	19.1	9.2	45.0	12.8	16.0	8.1	9.5	33.4
+ Mixup	17.7	8.5	25.2	16.4	27.2	9.5	11.7	25.4
+ Rsmix	21.3	9.9	54.3	12.0	<u>14.3</u>	7.9	8.9	41.9
+ PointDR	<u>17.3</u>	9.2	33.3	10.9	16.0	8.0	10.3	33.1
CurveNet	24.4	8.9	22.9	17.3	22.3	52.1	28.7	18.9
+ CutMix-R	13.8	9.1	18.2	11.1	15.5	8.1	<u>11.0</u>	22.4
+ CutMix-K	15.8	8.7	30.6	12.9	10.3	8.5	15.5	23.9
+ Mixup	19.3	<u>8.6</u>	17.9	21.6	19.8	25.7	20.1	21.4
+ Rsmix	16.9	9.1	35.0	11.0	<u>10.2</u>	9.2	13.1	30.9
+ PGD	22.7	16.8	11.2	12.9	26.0	48.9	25.3	18.3
+ PointDR	<u>13.7</u>	10.3	19.0	<u>10.3</u>	11.0	<u>7.6</u>	15.5	<u>22.0</u>
PCT	25.8	<u>9.0</u>	27.1	15.0	24.1	40.3	42.9	22.2
+ CutMix-R	12.7	10.1	14.5	9.8	14.3	8.3	10.9	20.7
+ CutMix-K	14.1	9.5	22.3	11.3	10.2	8.5	15.6	21.2
+ Mixup	18.1	9.4	15.6	15.8	18.2	23.5	22.8	21.1
+ Rsmix	15.2	9.3	25.7	10.2	10.0	8.7	13.0	29.8
+ PGD	20.0	14.6	10.5	16.9	24.8	29.5	22.7	21.2
+ WOLFmix	12.7	9.4	27.0	<u>9.4</u>	10.2	8.8	13.9	10.5
+ PointDR	12.5	9.9	16.2	11.0	14.4	<u>7.5</u>	<u>7.5</u>	21.1

Table 3: Comparison of mER on PointCloud-C between PointDR and state-of-the-art point cloud enhancement methods across three 3D deep models.

Method	mER	Scale	Jitter	Drop-G	Drop-L	Add-G	Add-L	Rotate
PointNet++	73.9	64.9	80.7	77.9	78.5	71.6	71.1	72.4
+ CutMix-R	64.9	62.9	72.2	62.8	67.2	59.3	58.1	71.8
+ CutMix-K	64.8	60.9	76.1	65.6	64.6	57.7	60.1	68.8
+ Mixup	62.8	<u>59.3</u>	<u>67.1</u>	64.1	69.2	57.8	<u>57.2</u>	<u>65.3</u>
+ Rsmix	66.7	63.8	78.1	66.2	68.1	59.4	60.6	70.6
+ PointDR	<u>62.4</u>	59.9	72.0	<u>58.6</u>	<u>64.1</u>	<u>56.8</u>	57.8	67.7
PCT	69.8	59.3	71.3	60.4	68.7	83.0	80.6	65.5
+ CutMix-R	<u>60.8</u>	59.5	62.9	58.8	60.8	57.7	61.2	64.7
+ CutMix-K	61.4	57.3	65.8	62.8	<u>58.8</u>	<u>56.3</u>	65.1	<u>63.5</u>
+ Mixup	62.7	57.6	62.0	58.9	63.6	65.7	67.5	<u>63.5</u>
+ Rsmix	63.3	59.2	70.5	60.6	59.8	58.6	65.9	68.5
+ PGD	65.6	65.7	<u>61.5</u>	66.7	71.8	62.6	64.3	66.7
+ PointDR	<u>60.8</u>	60.5	65.1	<u>58.1</u>	60.9	57.7	<u>57.5</u>	66.0
CurveNet	67.9	59.4	67.7	63.0	68.7	80.4	70.4	65.9
+ CutMix-R	63.2	61.0	68.2	59.8	65.4	58.6	61.7	68.0
+ CutMix-K	60.3	57.3	69.1	59.7	56.0	53.2	63.4	63.4
+ Mixup	62.5	<u>57.7</u>	62.7	60.9	<u>65.7</u>	64.1	61.7	<u>64.6</u>
+ Rsmix	62.2	59.2	73.5	57.4	59.5	56.5	61.9	67.8
+ PGD	67.4	68.9	62.8	59.2	69.1	75.5	67.2	69.3
+ PointDR	57.9	58.1	61.4	55.0	56.0	54.1	56.6	64.0

Table 4: Comparison of mER on OmniObject-C between PointDR and state-of-the-art point cloud enhancement methods across three 3D deep models.

Resampling	Downsampling	PCT	CurveNet
RSS	FPS FFPS WD	MNC PCC	MNC PCC
		✓	19.2 14.8 22.7 20.1
✓	✓		16.8 13.3 16.3 14.1
✓	✓		17.0 13.3 16.0 13.8
✓	✓	✓	15.8 12.5 15.8 13.7

Table 5: Ablation study based on mER with different sampling protocols in training. RSS refers to randomized size sampling; FFPS represents the filtered FPS; WD is the proposed weighted downsampling.

$\Delta N > 0$	$\Delta N < 0$	PCT	CurveNet
SI LG	RD KNN \tilde{k} NN	MNC PCC	MNC PCC
✓		✓	15.8 12.6 17.2 14.7
	✓		17.0 13.4 16.7 14.8
	✓	✓	17.2 13.8 17.4 15.9
✓		✓	15.8 12.5 15.8 13.7

Table 6: Ablation study based on mER of resampling protocols using different techniques for adding ($\Delta N > 0$) and removing points ($\Delta N < 0$). SI represents tangent plane up-sampling with random directions and distances (Huang et al. 2022). LG denotes the proposed local-geometry-preserved up-sampling detailed in Algorithm 1. RD refers to the random removal of points while KNN involves removing points within a fixed KNN range. \tilde{k} NN represents the proposed stochastic data augmentation strategy.

C (PCC) (Ren et al. 2022). Further details on implementation and hyperparameters are provided in the supplementary materials.

Sampling Protocols in Training. We compared various sampling protocols during the training phase. As shown in Table 5, the combination of randomized size sampling (RSS) and stochastic downsampling consistently delivers the best performance. removing RSS or substituting the proposed downsampling method with FPS significantly degrades the results. Notably, FFPS achieves the second-based performance, highlighting the importance of point reweighting.

Random Size Sampling. We investigate the impact of various resampling techniques during training. As shown in Table 6, we explore different methods for increasing and reducing sample sizes. The results indicate that the proposed \tilde{k} NN method plays a crucial role in enhancing performance. This suggests that stochastically determining the localness of the point dropping, *i.e.*, neighbor size, can improve robustness against corruptions. Additionally, we compare our up-sampling method in Algorithm 1 with Shape-invariant perturbation (SI), which conducts per-point perturbation on the tangent plane (Huang et al. 2022). The superiority of our method over SI shows that perturbation direction based on neighbor points preserves more local information than random directions.

Effect of Quantile-based Threshold ω of FFPS. As il-

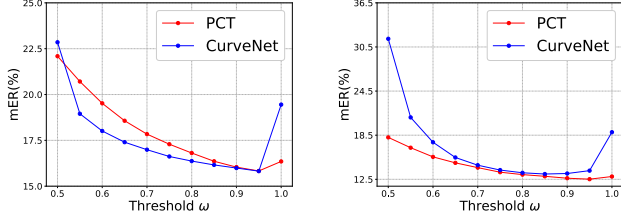


Figure 3: mERs of FFPS’s different threshold ω on ModelNet40-C (left) and PointCloud-C (right).

illustrated in Figure 3, retain 95% of the points (i.e., filtering out the 5% of points with the smallest weights) results in the best performance. Moreover, when nearly half of the points are removed, the mER peaks, likely due to the loss of critical information within the point cloud. As the number of removed points decreases, the error rate also decreases, reaching its lowest when about 5% of the points are filtered out, before rising again. This suggests that an optimal balance is achieved at this point.

4.4 Visualization Study

Isolation Rate. In Figure 4, we visualize the distribution of point-wise isolation rates for three example objects. The proposed rate effectively identifies boundary points and outliers, thereby enhancing subsequent point cloud sampling and improving learning robustness against corruption.

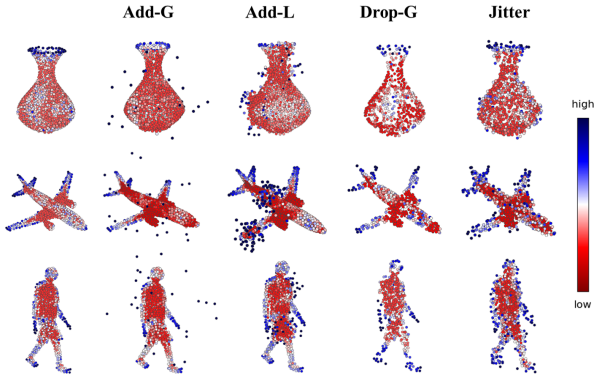


Figure 4: Visualization of point-wise *Isolation Rate*. Column 1 presents the clean data, while Columns 2 to 5 depict data with the corresponding corruption types indicated above each column.

Local-geometry-preserved Interpolation. Figure 5 visually compares the results of three upsampling techniques on four example objects. It is evident that both Jitter and SI (Huang et al. 2022) struggle with corrupted data, particularly when it is sparse and non-uniform. In contrast, the proposed LG method effectively combines completion and uniformity in the upsampling process.

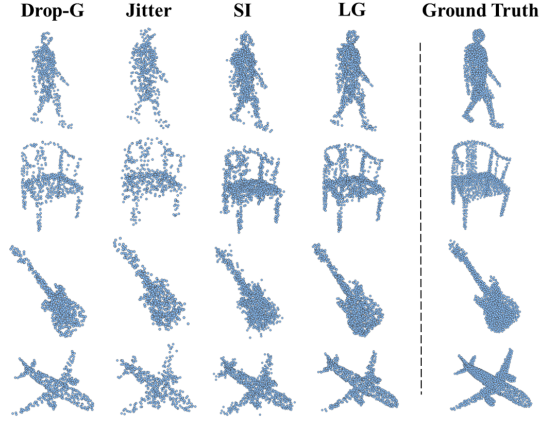


Figure 5: Visual comparison of three sampling techniques: (1) Jitter, (2) SI: tangent plane upsampling with random directions and distances (Huang et al. 2022), and (3) LG: the proposed local-geometry-preserved upsampling. The first column shows the corrupted data from PointCloud-C, while the last column presents the corresponding clean data.

Neighborhood Size \tilde{k} in Resampling. Stochastically determining the sample size is a critical aspect of the resampling protocol, driven by the stochastic neighborhood size \tilde{k} . As shown in Figure 6, a smaller \tilde{k} leads to local drops (second row), while a larger \tilde{k} results in more global removals (last row). A stochastic \tilde{k} would closely mimic real-world corruption, contributing to the robust improvement of the proposed protocol.

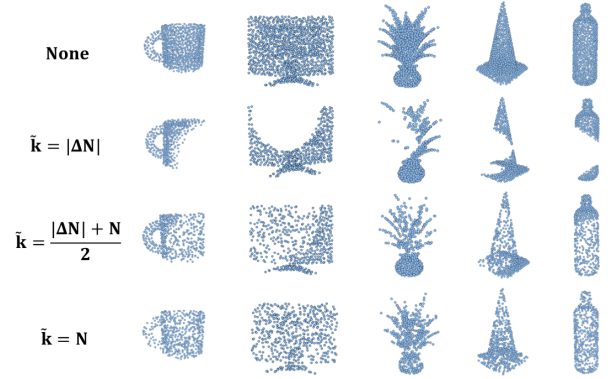


Figure 6: Visualization of samples with different neighborhood size \tilde{k} in resampling protocol.

5 Conclusion

This work focuses on the safety issue of 3D point cloud deep learning. It indicates that the current sampling protocol is not optimized for corrupted 3D point cloud analysis, thus posing a potential threat to 3D applications. Therefore, we introduce PointDR, an enhanced sampling protocol for point

clouds, addressing shortcomings in handling real-world corruptions. By incorporating point reweighting and tangent plane interpolation, our protocol mitigates outliers and restores incomplete point clouds without additional training or architectural changes. Extensive experiments show PointDR significantly improves robustness in 3D classification, outperforming state-of-the-art methods. This approach paves the way for more reliable 3D deep learning in critical areas like autonomous driving. Future research could extend this protocol to 3D scene-based datasets and higher-level tasks.

References

- Alexa, M.; Behr, J.; Cohen-Or, D.; Fleishman, S.; Levin, D.; and Silva, C. T. 2003. Computing and rendering point set surfaces. *IEEE Transactions on visualization and computer graphics*, 9(1): 3–15.
- Chen, Y.; Hu, V. T.; Gavves, E.; Mensink, T.; Mettes, P.; Yang, P.; and Snoek, C. G. 2020. Pointmixup: Augmentation for point clouds. In *Computer Vision—ECCV 2020: 16th European Conference, Glasgow, UK, August 23–28, 2020, Proceedings, Part III* 16, 330–345. Springer.
- Dai, P.; Zhang, Y.; Li, Z.; Liu, S.; and Zeng, B. 2020. Neural point cloud rendering via multi-plane projection. In *Proceedings of the IEEE/CVF Conference on Computer Vision and Pattern Recognition*, 7830–7839.
- Dong, X.; Chen, D.; Zhou, H.; Hua, G.; Zhang, W.; and Yu, N. 2020. Self-robust 3d point recognition via gather-vector guidance. In *2020 IEEE/CVF conference on computer vision and pattern recognition (cvpr)*, 11513–11521. IEEE.
- Dovrat, O.; Lang, I.; and Avidan, S. 2019. Learning to sample. In *Proceedings of the IEEE/CVF Conference on Computer Vision and Pattern Recognition*, 2760–2769.
- Eldar, Y.; Lindenbaum, M.; Porat, M.; and Zeevi, Y. Y. 1997. The farthest point strategy for progressive image sampling. *IEEE transactions on image processing*, 6(9): 1305–1315.
- Goyal, A.; Law, H.; Liu, B.; Newell, A.; and Deng, J. 2021. Revisiting point cloud shape classification with a simple and effective baseline. In *International Conference on Machine Learning*, 3809–3820. PMLR.
- Guo, M.-H.; Cai, J.-X.; Liu, Z.-N.; Mu, T.-J.; Martin, R. R.; and Hu, S.-M. 2021. Pct: Point cloud transformer. *Computational Visual Media*, 7: 187–199.
- Guo, Y.; Wang, H.; Hu, Q.; Liu, H.; Liu, L.; and Bennamoun, M. 2020. Deep learning for 3d point clouds: A survey. *IEEE Transactions on Pattern Analysis and Machine Intelligence*, 43(12): 4338–4364.
- He, Y.; Tang, D.; Zhang, Y.; Xue, X.; and Fu, Y. 2023a. Grad-pu: Arbitrary-scale point cloud upsampling via gradient descent with learned distance functions. In *Proceedings of the IEEE/CVF Conference on Computer Vision and Pattern Recognition*, 5354–5363.
- He, Y.; Tang, D.; Zhang, Y.; Xue, X.; and Fu, Y. 2023b. Grad-pu: Arbitrary-scale point cloud upsampling via gradient descent with learned distance functions. In *Proceedings of the IEEE/CVF Conference on Computer Vision and Pattern Recognition*, 5354–5363.
- Hong, C.-Y.; Chou, Y.-Y.; and Liu, T.-L. 2023. Attention discriminant sampling for point clouds. In *Proceedings of the IEEE/CVF International Conference on Computer Vision*, 14429–14440.
- Hu, Q.; Yang, B.; Xie, L.; Rosa, S.; Guo, Y.; Wang, Z.; Trigoni, N.; and Markham, A. 2020. Randla-net: Efficient semantic segmentation of large-scale point clouds. In *Proceedings of the IEEE/CVF conference on computer vision and pattern recognition*, 11108–11117.
- Huang, H.; Li, D.; Zhang, H.; Ascher, U.; and Cohen-Or, D. 2009. Consolidation of unorganized point clouds for surface reconstruction. *ACM transactions on graphics (TOG)*, 28(5): 1–7.
- Huang, H.; Wu, S.; Gong, M.; Cohen-Or, D.; Ascher, U.; and Zhang, H. 2013. Edge-aware point set resampling. *ACM transactions on graphics (TOG)*, 32(1): 1–12.
- Huang, Q.; Dong, X.; Chen, D.; Zhou, H.; Zhang, W.; and Yu, N. 2022. Shape-invariant 3d adversarial point clouds. In *Proceedings of the IEEE/CVF conference on computer vision and pattern recognition*, 15335–15344.
- Kim, S.; Lee, S.; Hwang, D.; Lee, J.; Hwang, S. J.; and Kim, H. J. 2021. Point cloud augmentation with weighted local transformations. In *Proceedings of the IEEE/CVF international conference on computer vision*, 548–557.
- Lang, I.; Manor, A.; and Avidan, S. 2020. Samplenet: Differentiable point cloud sampling. In *Proceedings of the IEEE/CVF Conference on Computer Vision and Pattern Recognition*, 7578–7588.
- Lee, D.; Lee, J.; Lee, J.; Lee, H.; Lee, M.; Woo, S.; and Lee, S. 2021. Regularization strategy for point cloud via rigidly mixed sample. In *Proceedings of the IEEE/CVF Conference on Computer Vision and Pattern Recognition*, 15900–15909.
- Li, R.; Li, X.; Heng, P.-A.; and Fu, C.-W. 2020. Pointaugment: an auto-augmentation framework for point cloud classification. In *Proceedings of the IEEE/CVF conference on computer vision and pattern recognition*, 6378–6387.
- Lipman, Y.; Cohen-Or, D.; Levin, D.; and Tal-Ezer, H. 2007. Parameterization-free projection for geometry reconstruction. *ACM Transactions on Graphics (ToG)*, 26(3): 22–es.
- Liu, H.; Jia, J.; and Gong, N. Z. 2021. Pointguard: Provably robust 3d point cloud classification. In *Proceedings of the IEEE/CVF conference on computer vision and pattern recognition*, 6186–6195.
- Liu, Y.; Fan, B.; Xiang, S.; and Pan, C. 2019. Relation-shape convolutional neural network for point cloud analysis. In *Proceedings of the IEEE/CVF conference on computer vision and pattern recognition*, 8895–8904.
- Lv, C.; Lin, W.; and Zhao, B. 2021. Approximate intrinsic voxel structure for point cloud simplification. *IEEE Transactions on Image Processing*, 30: 7241–7255.
- Nezhadarya, E.; Taghavi, E.; Razani, R.; Liu, B.; and Luo, J. 2020. Adaptive hierarchical down-sampling for point cloud classification. In *Proceedings of the IEEE/CVF Conference on Computer Vision and Pattern Recognition*, 12956–12964.

- Qi, C. R.; Su, H.; Mo, K.; and Guibas, L. J. 2017a. Pointnet: Deep learning on point sets for 3d classification and segmentation. In *Proceedings of the IEEE conference on computer vision and pattern recognition*, 652–660.
- Qi, C. R.; Yi, L.; Su, H.; and Guibas, L. J. 2017b. Pointnet++: Deep hierarchical feature learning on point sets in a metric space. *Advances in neural information processing systems*, 30.
- Qian, G.; Li, Y.; Peng, H.; Mai, J.; Hammoud, H.; Elhoseiny, M.; and Ghanem, B. 2022. Pointnext: Revisiting pointnet++ with improved training and scaling strategies. *Advances in Neural Information Processing Systems*, 35: 23192–23204.
- Qian, Y.; Hou, J.; Kwong, S.; and He, Y. 2020. PUGeoNet: A geometry-centric network for 3D point cloud upsampling. In *European conference on computer vision*, 752–769. Springer.
- Qian, Y.; Hou, J.; Zhang, Q.; Zeng, Y.; Kwong, S.; and He, Y. 2023. Task-Oriented Compact Representation of 3D Point Clouds via A Matrix Optimization-Driven Network. *IEEE Transactions on Circuits and Systems for Video Technology*, 33(11): 6981–6995.
- Qiu, S.; Anwar, S.; and Barnes, N. 2022. Pu-transformer: Point cloud upsampling transformer. In *Proceedings of the Asian conference on computer vision*, 2475–2493.
- Ren, J.; Kong, L.; Pan, L.; and Liu, Z. 2022. Pointcloud-c: Benchmarking and analyzing point cloud perception robustness under corruptions. *preprint*, 3.
- Sotoodeh, S. 2006. Outlier detection in laser scanner point clouds. *International Archives of the Photogrammetry, Remote Sensing and Spatial Information Sciences*, 36(5): 297–302.
- Sun, J.; Cao, Y.; Choy, C. B.; Yu, Z.; Anandkumar, A.; Mao, Z. M.; and Xiao, C. 2021. Adversarially robust 3d point cloud recognition using self-supervisions. *Advances in Neural Information Processing Systems*, 34: 15498–15512.
- Sun, J.; Koenig, K.; Cao, Y.; Chen, Q. A.; and Mao, Z. M. 2020. On adversarial robustness of 3d point cloud classification under adaptive attacks. *arXiv preprint arXiv:2011.11922*.
- Sun, J.; Zhang, Q.; Kailkhura, B.; Yu, Z.; Xiao, C.; and Mao, Z. M. 2022. Modelnet40-c: A robustness benchmark for 3d point cloud recognition under corruption. In *ICLR 2022 Workshop on Socially Responsible Machine Learning*, volume 7.
- Uy, M. A.; Pham, Q.-H.; Hua, B.-S.; Nguyen, T.; and Yeung, S.-K. 2019. Revisiting point cloud classification: A new benchmark dataset and classification model on real-world data. In *Proceedings of the IEEE/CVF international conference on computer vision*, 1588–1597.
- Wang, Y.; Sun, Y.; Liu, Z.; Sarma, S. E.; Bronstein, M. M.; and Solomon, J. M. 2019. Dynamic graph cnn for learning on point clouds. *ACM Transactions on Graphics (tog)*, 38(5): 1–12.
- Wu, S.; Huang, H.; Gong, M.; Zwicker, M.; and Cohen-Or, D. 2015a. Deep points consolidation. *ACM Transactions on Graphics (ToG)*, 34(6): 1–13.
- Wu, T.; Zhang, J.; Fu, X.; Wang, Y.; Ren, J.; Pan, L.; Wu, W.; Yang, L.; Wang, J.; Qian, C.; et al. 2023. Omniobject3d: Large-vocabulary 3d object dataset for realistic perception, reconstruction and generation. In *Proceedings of the IEEE/CVF Conference on Computer Vision and Pattern Recognition*, 803–814.
- Wu, Z.; Duan, Y.; Wang, H.; Fan, Q.; and Guibas, L. J. 2020. If-defense: 3d adversarial point cloud defense via implicit function based restoration. *arXiv preprint arXiv:2010.05272*.
- Wu, Z.; Song, S.; Khosla, A.; Yu, F.; Zhang, L.; Tang, X.; and Xiao, J. 2015b. 3d shapenets: A deep representation for volumetric shapes. In *Proceedings of the IEEE conference on computer vision and pattern recognition*, 1912–1920.
- Xiang, T.; Zhang, C.; Song, Y.; Yu, J.; and Cai, W. 2021. Walk in the cloud: Learning curves for point clouds shape analysis. In *Proceedings of the IEEE/CVF international conference on computer vision*, 915–924.
- Xu, M.; Zhang, J.; Zhou, Z.; Xu, M.; Qi, X.; and Qiao, Y. 2021. Learning geometry-disentangled representation for complementary understanding of 3d object point cloud. In *Proceedings of the AAAI conference on artificial intelligence*, volume 35, 3056–3064.
- Yan, X.; Zheng, C.; Li, Z.; Wang, S.; and Cui, S. 2020. Pointasnl: Robust point clouds processing using nonlocal neural networks with adaptive sampling. In *Proceedings of the IEEE/CVF conference on computer vision and pattern recognition*, 5589–5598.
- Ye, S.; Chen, D.; Han, S.; Wan, Z.; and Liao, J. 2021. Meta-PU: An arbitrary-scale upsampling network for point cloud. *IEEE transactions on visualization and computer graphics*, 28(9): 3206–3218.
- Yifan, W.; Wu, S.; Huang, H.; Cohen-Or, D.; and Sorkine-Hornung, O. 2019. Patch-based progressive 3d point set upsampling. In *Proceedings of the IEEE/CVF Conference on Computer Vision and Pattern Recognition*, 5958–5967.
- Ying, X.; Xin, S.-Q.; Sun, Q.; and He, Y. 2013. An intrinsic algorithm for parallel poisson disk sampling on arbitrary surfaces. *IEEE transactions on visualization and computer graphics*, 19(9): 1425–1437.
- Yu, L.; Li, X.; Fu, C.-W.; Cohen-Or, D.; and Heng, P.-A. 2018a. Ec-net: an edge-aware point set consolidation network. In *Proceedings of the European conference on computer vision (ECCV)*, 386–402.
- Yu, L.; Li, X.; Fu, C.-W.; Cohen-Or, D.; and Heng, P.-A. 2018b. Pu-net: Point cloud upsampling network. In *Proceedings of the IEEE conference on computer vision and pattern recognition*, 2790–2799.
- Yu, X.; Tang, L.; Rao, Y.; Huang, T.; Zhou, J.; and Lu, J. 2022. Point-bert: Pre-training 3d point cloud transformers with masked point modeling. In *Proceedings of the IEEE/CVF conference on computer vision and pattern recognition*, 19313–19322.
- Zhang, J.; Chen, L.; Ouyang, B.; Liu, B.; Zhu, J.; Chen, Y.; Meng, Y.; and Wu, D. 2022a. Pointcutmix: Regularization strategy for point cloud classification. *Neurocomputing*, 505: 58–67.

Zhang, Y.; Zhao, W.; Sun, B.; Zhang, Y.; and Wen, W. 2022b. Point cloud upsampling algorithm: A systematic review. *Algorithms*, 15(4): 124.

Zhou, H.; Chen, K.; Zhang, W.; Fang, H.; Zhou, W.; and Yu, N. 2019. Dup-net: Denoiser and upsampler network for 3d adversarial point clouds defense. In *Proceedings of the IEEE/CVF international conference on computer vision*, 1961–1970.

Zhu, Q.; Fan, L.; and Weng, N. 2024. Advancements in point cloud data augmentation for deep learning: A survey. *Pattern Recognition*, 110532.